Special Issue Article

Institution of MECHANICAL ENGINEERS
Journal of ENGINEERING MANUFACTURE

Proc IMechE Part B:
J Engineering Manufacture
2021, Vol. 235(14) 2273–2287

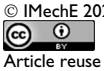
Article reuse guidelines:
sagepub.com/journals-permissions
DOI: 10.1177/0954405420968161
journals.sagepub.com/home/pib
SAGE

An integrated analysis of productivity, hole quality and cost estimation of single-pulse laser drilling process

Shoaib Sarfraz[1], Essam Shehab[1], Konstantinos Salonitis[1], Wojciech Suder[1], Misbah Niamat[2] and Muhammad Jamil[3]

Abstract

Laser drilling is a well-established manufacturing process utilised to produce holes in various aeroengine components. This research presents an experimental investigation on the effects of laser drilling process parameters on productivity (material removal rate), hole quality (hole taper) and drilling cost. Single-pulse drilling was employed to drill a thin-walled Inconel 718 superalloy plate of 1 mm thickness using pulsed Nd:YAG laser. The experiments were designed using Box-Behnken statistical approach to investigate the impacts of pulse energy, pulse duration, gas pressure and gas flow rate on the selected responses. Multi-objective optimisation was performed using response surface methodology (RSM) based grey rational analysis (GRA) to identify optimal drilling conditions aiming to maximise the MRR and minimise hole taper and drilling cost. The optimal combination of drilling parameters was found as pulse energy of 20 J, pulse duration of 6 ms, gas pressure of 100 psi and gas flow rate of 40 mm^3/s. A detailed cost analysis identified labour cost, gas consumption and machine costs as the major cost elements of the laser drilling process.

Keywords

Laser drilling, single-pulse, material removal rate, cost, hole taper, multi-objective optimisation

Date received: 6 March 2020; accepted: 27 September 2020

Introduction

Lucrative properties of Inconel 718 (IN 718) have made it the best candidate material for the aerospace industry owing to its high strength, wear and fatigue resistance at elevated temperatures. A significant application involves the use of IN 718 in aeroengine components used in high-temperature applications. The operating temperature of these components ranges between 400 and 1100°C.[1] Substantial cooling is necessary to increase the operational life of these components. Therefore, a large number of holes are produced, which serve as a passage for the air coolant in hot path components. In the last few decades, an increase in the number of cooling holes in turbine design has been observed to improve the performance and efficiency of aeroengine. For instance, 40,000 holes are drilled in the afterburner of a gas turbine.[2] However, this material is difficult to manufacture using conventional machining processes because of higher tool wear and low material removal rate.[3]

Laser drilling has been extensively adopted for producing cooling holes for aerospace gas turbine components, such as combustion chambers, high-pressure turbine blades and nozzle guide vanes.[4] It is a non-contact and high-speed drilling process used for the manufacture of small and precise holes in almost any material, such as metals, alloys, ceramics and composites. In the laser drilling process, a high power laser beam is directed on the workpiece surface, where the optical energy of the laser beam is thermalised and rapidly heats the base material. Some of the energy is lost due to scattering and reflection of the laser beam. Depending on laser intensity, the material is removed in

[1]Manufacturing Department, School of Aerospace, Transport and Manufacturing, Cranfield University, Cranfield, Bedfordshire, UK
[2]Mechanical Engineering Department, Muhammad Nawaz Sharif University of Engineering and Technology, Multan, Pakistan
[3]College of Mechanical and Electrical Engineering, Nanjing University of Aeronautics and Astronautics, Nanjing, China

Corresponding author:
Shoaib Sarfraz, Manufacturing Department, School of Aerospace, Transport and Manufacturing, Cranfield University, Research Area A, Manufacturing Department, Cranfield, Bedfordshire MK43 0AL, UK.
Email: shoaib.sarfraz@cranfield.ac.uk

both the liquid and/or vapour state. Plasma and recoil pressure normally appear in laser drilling due to the high intensities used in the process[5] which help in the expulsion of molten metal and result in the formation of a hole cavity (Figure 1(a)). Assist gas is also used to remove the melt and/or vapours from the hole, as shown in Figure 1(b). The assist gas pressure together with the plasma and recoil pressure control material ejection in the laser drilling process.[6,7]

Different types of laser drilling techniques are available to perform the drilling operation. Gautam and Pandey[8] classified these techniques into static and dynamic drilling based on relative movement between the work part and the laser beam. Single-shot/single-pulse laser drilling and percussion drilling are examples of static drilling where the removal of material is carried out by the effect of several pulses with both the laser beam and the work part in a stable condition. On the other hand, in dynamic drilling, the hole is initially pierced into the centre of the substrate with a laser beam followed by beam rotation towards the circumference of the hole. Trepanning and helical drilling fall into this category. Single-pulse drilling produces holes using only one shot and is the fastest method to drill holes in a material. With single-pulse drilling, drilling time can be reduced but at the expense of hole quality; on the other hand, trepanning gives good hole quality but the drilling time is higher. This shows that there is a trade-off between the quality and drilling time.

The laser drilling process is associated with some undesirable defects, such as micro-cracks, heat affected zone, hole taper, spatter and recast layer that needs to be minimised.[9] Taper formation is an inherent characteristic of laser material processing. It is an essential attribute that significantly influences the drilled hole quality. Zero or lower hole taper is always desirable specifically in aeroengine components where close tolerances and high quality are strict requirements.[10] Hole taper is affected by several factors, such as laser beam characteristics, types of drilling methods applied and laser processing parameters.[11] The characteristics of a laser beam depend upon the laser optic or hardware components used to deliver the laser beam from the laser source to the workpiece. These components include mirrors, beam splitters, fibres, collimators, focus heads etc. Special optics are needed to achieve holes with a minimum taper angle, which is out of the scope of this study. The laser processing parameters which affect hole taper include laser pulse duration/width, pulse energy, assist gas pressure, beam focal position and gas flow rate.[12–20] In previous research studies, several authors have explored the effects of these process parameters for single-pulse drilling. Yilbas and Yilbas[21] used the full factorial method to evaluate the impacts of focal position and material thickness on the quality of laser-drilled holes in Nimonic 75. In another study, Yilbas[22] examined the

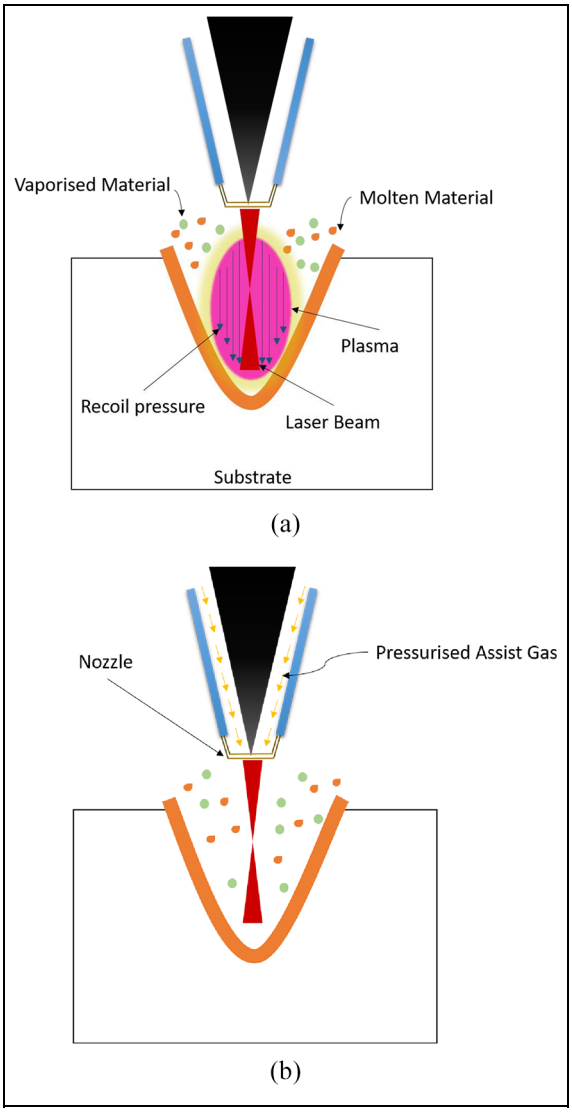

Figure 1. Schematic of the laser drilling process: (a) vapour driven melt expulsion and (b) assist gas melt expulsion.

effects of pulse duration, pulse energy, workpiece thickness and focal length on hole quality by comparing different materials (titanium, nickel and stainless steel). All process parameters were found to affect hole quality significantly. Sarfraz et al.[15] evaluated the influence of process parameters (pulse duration and pulse energy) on hole taper during laser drilling of IN 718 alloy. The results revealed that hole taper is significantly influenced by pulse duration and pulse energy. Variations in hole diameter were investigated by Rodden et al.[23] during laser drilling of carbon fibre composites. The exit hole diameter was found to be a function of material thickness and pulse energy. Yilbas and Aleem[24] examined the impacts of single-pulse laser drilling on the hole quality in Tantalum. The selected parameters were pulse energy, assist gas pressure, lens focal position and workpiece thickness. It was observed that all applied parameters significantly influence hole

quality. The impact of peak power and pulse duration on hole taper was studied by Kacar et al.[25] A significant influence was observed on hole taper with an increase in peak power and pulse duration. Xiao et al.[26] and Zhang et al.[27] investigated the influence of various process parameters on hole taper and the heat-affected zone, and recast layer respectively. It was revealed that hole quality could be enhanced when proper selection and control of process parameters is applied.

Productivity is also an important feature of the manufacturing process besides hole quality. The parameters which affect productivity include pulse width, gas pressure, gas flow rate and pulse energy.[19,28–30] Panda et al.[19] examined the impact of the laser drilling process parameters, including pulse duration, gas pressure, number of pulses, and gas flow rate on the material removal rate and hole quality. It has been shown that variation in the process parameters significantly affects MRR and hole quality. Priyadarshini et al.[30,31] extended this work to optimise the hole quality and MRR using grey-fuzzy and fuzzy-TOPSIS methods. The influence of pulse energy and pulse duration on hole quality and material removal rate was examined by Sarfraz et al.[15] The results revealed that both productivity and hole quality is greatly influenced by the control of applied parameters.

Cost is a key factor being considered in every industry and has a significant impact on product outcomes because of the global competitive market. Various researchers have estimated the operating cost associated with different laser machining processes. Benyounis et al.[32] and Eltawahni et al.[33] estimated the operating costs of laser welding and laser cutting along with the product quality. The authors used Response Surface Methodology (RSM) to investigate the impact of process parameters and find out the optimal combination of process parameters at minimum cost and maximum quality. A significant influence of process parameters was observed on both the operating cost and quality. Recently, Sarfraz et al.[34] reported that the process parameters affecting the performance of the laser drilling process also have a substantial impact on the cost that needs to be investigated.

A holistic literature review shows that the productivity and the product quality of laser drilling have had little attention from researchers. However, there is no research work available discussing the cost of the laser drilling process. This research contributes to an evaluation of the influence of the laser drilling process parameters improving the material removal rate and hole quality while minimising the drilling cost. A comprehensive statistical analysis has been performed to evaluate the effects of the process parameters. Empirical models have been developed successfully to predict output responses. The adequacy of developed models has been verified through analysis of variance (ANOVA). Furthermore, multi-objective optimisation has been applied to achieve the best combination of laser drilling parameters for optimum response values. A detailed cost analysis has also been performed to explore the economic implications of the laser drilling process.

Table 1. Chemical composition of the material in wt%.

Ni	Cr	Mo	Mn	Ti	Nb	Fe	Al	Si
52.56	19	3.05	0.18	0.9	5.13	18.5	0.5	0.18

Materials, equipment and methods

The samples of IN 718 plates of 100 mm × 100 mm × 1.0 mm dimensions were procured from Goodfellow, UK. The chemical composition of the material was validated via optical emission spectroscopy, the results of which are provided in Table 1.

The drilling operation was performed using a flash lamp-pumped Nd:YAG laser (JK300HPS model, JK Lasers, UK). Laser system specifications are presented in Appendix 1. All experiments were conducted at a laser beam incidence angle of 90° to the material surface. The focal position of the laser beam was maintained at the workpiece surface using a 300 mm focal length lens, giving a spot diameter of 0.9 mm. The laser beam profile distribution was Gaussian with TEM_{00}. Conical nozzle with a diameter of 2.0 mm was used to deliver the assist gas, and the distance between the nozzle tip and the substrate was fixed at 3.0 mm. Compressed air was employed as an assist gas. Gas pressure and gas flow rate were controlled through a gas regulator and gas flow meter installed on the cylinder. The experimental setup and its schematic diagram are presented in Figure 2.

In order to analyse the influence of the process parameters on the material removal rate (MRR), drilling cost (C_d), and hole quality (H_T), response surface methodology was employed. Four laser drilling process parameters were selected, namely pulse energy, pulse duration, gas pressure and gas flow rate. These process parameters were chosen based on their influence on material removal rate, hole quality and drilling cost.[12,14,15,19,28–30,34] The selection of limits and their levels was based on trial experiments and literature review. Table 2 shows the controlled parameters along with the selected levels. Some of the parameters were kept constant and are also provided in Table 2.

A series of experiments was performed using the Box-Behnken experimental design technique. Overall 27 experiments were conducted with four process parameters and three centre points.[35] Each experimental run was replicated three times to assure the reproducibility and reliability of the experimental procedure. Figure 3 shows a photograph of the different experiments conducted; both the entry and exit sides of drilled holes are presented, where each row represents the repetition of experiments. The experimental runs with the observed response values are provided in Table 3. A similar

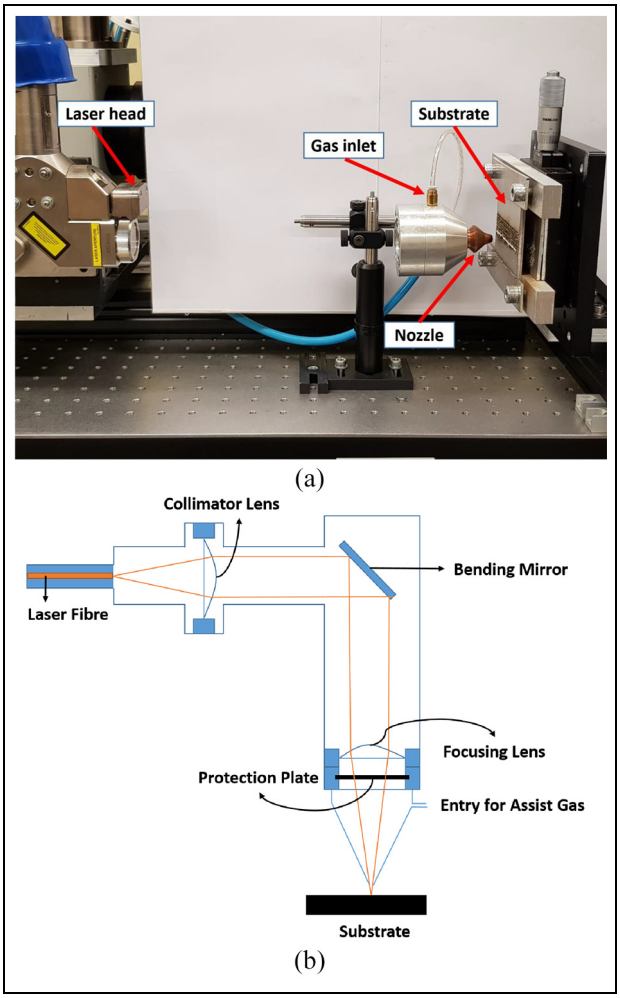

Figure 2. Laser drilling setup: (a) experimental and (b) schematic.

strategy was adopted to calculate the hole taper and material removal rate, as reported in previous work.[15] The detailed cost analysis is explained in the following section.

Cost estimation

Manufacturing cost estimation is an essential activity for companies targeting to become successful in the current competitive scenario. For this purpose, this research intends to provide a detailed cost analysis for the laser drilling process considering single-pulse laser drilling.

In order to highlight substantial cost components, material cost, labour cost, maintenance cost and equipment running cost are considered. The total cost is changed with a small modification to a single cost driver. Therefore, it is only possible to generate a comprehensive cost estimate for a particular process when all of its cost drivers are identified.[36]

The main cost drivers relevant to the laser drilling process have been determined through experts' opinion and literature review (see Appendix 2). Equipment running cost, maintenance, material and labour costs are the key drivers in laser drilling cost estimation. After a comprehensive study, it was identified that equipment running cost further includes equipment depreciation, electricity consumption, components replacement, gas consumption, component handling and overhead costs. When all cost drivers are finalised, a cost is allocated to each driver and the total process cost can be calculated.

Table 2. Levels of the process parameters.

Parameters	Levels
Pulse energy P_e, (J)	20, 30, 40
Pulse duration P_d, (ms)	6, 11, 16
(Assist) gas pressure G_p, (psi)	50, 75, 100
(Assist) gas flow rate G_{fr}, (l/min)	30, 35, 40
Material thickness (mm)	1.0
Nozzle diameter (mm)	2.0
Stand-off distance (mm)	3.0
Laser beam focal position	At workpiece surface

Laser drilling cost estimation

The total cost of laser drilling per hole (C_{ld}) consists of different cost components including the material cost, labour cost (C_{lr}), maintenance cost (C_{main}) and equipment running cost. The equipment running cost further consists of machine cost (C_{me}), electricity cost (C_{ey}), gas consumption cost (C_{gc}) and consumables cost (C_{con}). Since the focus of this study is to evaluate the process cost, therefore the material cost was classified as a fixed cost and the total drilling cost in cumulative form can be represented as the equation (1).

$$C_{ld} = C_{lr} + C_{me} + C_{ey} + C_{gc} + C_{con} + C_{main} \quad (1)$$

Labour cost. Labour cost per hole (C_{lr}) is comprised of direct labour cost and labour overhead, as shown in equation (2). Direct labour cost (C_{dl}) is calculated based on the wage rate of the operator, the number of operators required for the process and the drilling time. Labour's overhead (H_{lo}) includes training cost, medical and fringe benefits.[37] This is estimated as 40% of the direct labour cost. The total labour cost is expressed as equation (3).

$$C_{lr} = Direct\ labour\ cost(C_{dl}) + Labour\ over\ head(H_{lo}) \quad (2)$$

$$C_{lr} = \left(C_{hl} \times L_r \times \frac{T}{3600}\right) + \left[0.4\left(C_{hl} \times L_r \times \frac{T}{3600}\right)\right] \quad (3)$$

where C_{hl} is the hourly cost of labour taken as 15 £/hr for normal labour, L_r is the total number of labour involved during actual drilling and T is the drilling time per hole (s). Each hole has a specific drilling time,

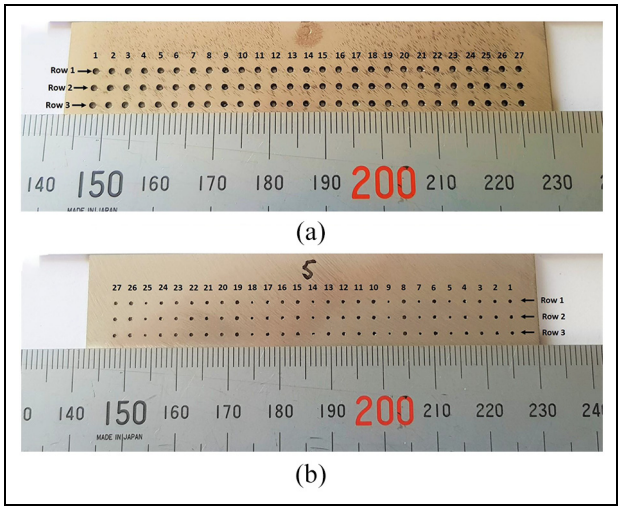

Figure 3. Arrays of holes after drilling: (a) entry side and (b) exit side.

changing drilling parameters vary the drilling time per hole.

Machine cost. Machine cost per hole includes the machine depreciation cost (C_{md}) and machine overhead (H_{mo}) (equation (4)). The machine depreciation cost is based on the equipment useful life (L_{ep}), its purchase cost (C_{ep}) and salvage value (can be omitted for laser machine), production hours per year (H_y), and the drilling time (T).

The machine cost (C_{me}) is calculated using equation (5),

$$C_{me} = \textit{Machine depreciation cost}(C_{md}) + \textit{Machine overhead}(H_{mo}) \quad (4)$$

$$C_{me} = \left(\frac{C_{ep}}{L_{ep} \times H_y} \times \frac{T}{3600}\right) + \left[0.3\left(\frac{C_{ep}}{L_{ep} \times H_y} \times \frac{T}{3600}\right)\right] \quad (5)$$

where C_{ep} is the purchase cost of equipment (laser & chiller) 61050 £, L_{ep} is the equipment useful life (12 years) and H_y is the production hours per year 1920 h (240 days/year × 8 h/day). Machine overhead includes lighting/HVAC and floor space cost that is, 30% of machine depreciation cost.[38]

Cost of electricity. Electricity cost comprises energy consumed by the equipment, the unit price of energy and the drilling time. Four factors were taken into consideration for the electrical energy consumption of equipment that is, electrical power of the chiller, electrical power of the laser, utilised laser power and the maximum power achieved by the laser. The cost of electricity (C_{ey}) per hole is represented by equation (6).

Table 3. Experimental layout and results.

Exp. No.	Process parameters				Responses		
	P_e (J)	P_d (ms)	G_p (psi)	G_{fr} (l/min)	MRR (mm^3/s)	H_T (deg)	C_d* (£)
1	30	11	50	30	105.4	17.22	0.01353
2	30	11	50	40	110	7.29	0.01473
3	30	6	50	35	127.6	11.94	0.00779
4	30	16	50	35	89.3	8.41	0.02709
5	20	11	50	35	94.6	12.71	0.01453
6	40	11	50	35	108.1	18.27	0.01667
7	20	6	75	35	118.2	7.91	0.00818
8	40	6	75	35	171.7	13.47	0.01233
9	20	16	75	35	100.9	8.38	0.02495
10	40	16	75	35	104	11.94	0.02442
11	30	11	75	35	122.9	11.15	0.01574
12	30	11	75	35	125.2	11.81	0.01384
13	30	11	75	35	128	11.93	0.01512
14	20	11	75	30	107.1	12.86	0.01163
15	40	11	75	30	133.4	18.42	0.01550
16	30	6	75	30	140.1	14.1	0.01128
17	30	16	75	30	111	12.56	0.01844
18	20	11	75	40	110.6	5.89	0.01492
19	40	11	75	40	141.4	10.74	0.02016
20	30	6	75	40	157	9.12	0.01138
21	30	16	75	40	106.8	5.59	0.03282
22	30	11	100	30	131.7	12.4	0.01492
23	30	6	100	35	145.5	7.77	0.01357
24	30	16	100	35	113	6.24	0.02633
25	20	11	100	35	115.4	8.54	0.01244
26	40	11	100	35	148.2	14.1	0.01628
27	30	11	100	40	133.1	5.07	0.01930

*Cost is multiplied by a factor of 100.

$$C_{ey} = \left[C_{up} \times \left(\left(\frac{P_l \times P_{ut}}{P_{max}}\right) + P_{ch}\right)\right] \times \frac{T}{3600} \quad (6)$$

where C_{up} is the unit price of electricity (0.14 £/kWh), P_l is the electrical power of the laser (10 kW), P_{ut} is the utilised laser power in kW ($P_e \times pulse\ frequency = J \times \frac{1}{s}$), P_{max} is the maximum power achieved by the laser (0.3 kW) and P_{ch} is the electrical power of the chiller (3.8 kW).

Cost of gas consumption. The cost of gas consumption per hole (C_{gc}) depends on the gas flow rate (measured using gas flow meter), the unit price of the gas and drilling time. In this work, compressed air was employed as an assist gas. Equation (7) presents the calculations used for the gas consumption cost.

$$C_{gc} = G_{fr} \times G_{up} \times 60 \times \frac{T}{3600} \quad (7)$$

where G_{fr} is the flow rate of gas in l/min (varies for each experiment) and G_{up} is the unit price of gas (0.00390 £/l for compressed air).

Cost of consumables. Consumable laser components (water filters, laser pumps) have a limited lifetime and need regular replacement. The consumables cost per hole (C_{con}) can be calculated based on the price of consumable components and their useful lifetime (equation (8)).

$$C_{con} = \left[\left(\frac{C_{wf}}{T_{wf}}\right) + \left(\frac{C_{lp}}{T_{lp}}\right)\right] \times \frac{T}{3600} \quad (8)$$

where C_{wf} is the price of water filters (300 £), T_{wf} is the (expected) lifetime of water filters (2000 h), C_{lp} is the price of laser pumps (500 £) and T_{lp} is the (expected) lifetime of laser pumps (1200 h).

Cost of maintenance. Pulsed Nd:YAG laser requires periodic maintenance and service. Therefore, maintenance cost depends on the hourly cost of maintenance labour, maintenance time required, available working time of machine and drilling time per hole, as shown in equation (9).

$$C_{main} = C_{lab-main} \times \frac{T_{main}}{T_{mac-work}} \times \frac{T}{3600} \quad (9)$$

where C_{main} is the maintenance cost per hole in £, $C_{lab-main}$ is the cost of labour for maintenance experts (100 £/hr), T_{main} is the time required for maintenance (24 h) and $T_{mac-work}$ is the (expected) available working time of the machine before breakdown (1920 h).

Total drilling cost. Labour cost C_{lr}, machine cost C_{me}, electricity cost C_{ey} (laser & chiller), gas consumption cost C_{gc}, consumables cost C_{con} and maintenance cost C_{main} are added to calculate the total drilling cost per hole. It is essential to mention that all cost components data has been acquired from the industry.

The percentage contribution of all cost components under low, medium and high levels of process parameters is provided in Figure 4. At the low level of parameters, labour cost was a maximum of 62% followed by gas consumption cost of 21%, machine cost of 10%, maintenance cost of 4%, electricity cost of 2% and consumable cost of 1% in the total drilling cost respectively (Figure 4(a)). A similar contribution of cost components was observed at medium and high levels of process parameters (Figure 4(b) and (c)). For the laser cutting process, Riveiro et al.[39] reported similar findings that showed gas consumption, machine (laser/chiller) cost and electricity cost as major cost components ignoring the labour cost.

Results and discussion

Mathematical modelling

Regression analysis was applied using Design Expert® (v10) to develop mathematical models for predicting output responses. The obtained mathematical models for MRR, hole taper and drilling cost are provided in equations (10) to (12), respectively.

$$\begin{aligned} MRR = &- 108.795 + (2.65783 \times P_e) + (11.02667 \times P_d) \\ &+ (1.54213 \times G_p) + (2.82433 \times G_{fr}) \\ &- (0.252 \times P_e \times P_d) + (0.0193 \times P_e \times G_p) \\ &- (0.211 \times P_d \times G_{fr}) - (0.010765 \times {G_p}^2) \end{aligned} \quad (10)$$

$$\begin{aligned} H_T = &+ 40.26228 - (0.58231 \times P_e) + (1.42259 \times P_d) \\ &- (0.072365 \times G_p) \\ &- (0.73091 \times G_{fr}) + (0.013962 \times {P_e}^2) \\ &- (0.073135 \times {P_d}^2) \end{aligned} \quad (11)$$

$$\begin{aligned} C_d = &+ 0.47025 + (0.00155714 \times P_e) - (0.060832 \times P_d) \\ &- (0.011044 \times G_{fr}) \\ &+ (0.00142821 \times P_d \times G_{fr}) + (0.00117125 \times {P_d}^2) \end{aligned} \quad (12)$$

The significance of process parameters and the developed mathematical models was confirmed through analysis of variance (ANOVA). The analysis results are provided in Appendix 3. These results show essential terms (with p values < 0.05) and the adequacy measures (R^2 and adjusted R^2). All process parameters were found as significant for MRR and hole taper; however, in the case of drilling cost three process parameters that is, pulse energy, pulse duration and gas flow rate were found to be the most contributing parameters. It is noted that the values of adequacy measures are close to 1, which provides proof of the adequacy of the developed models.

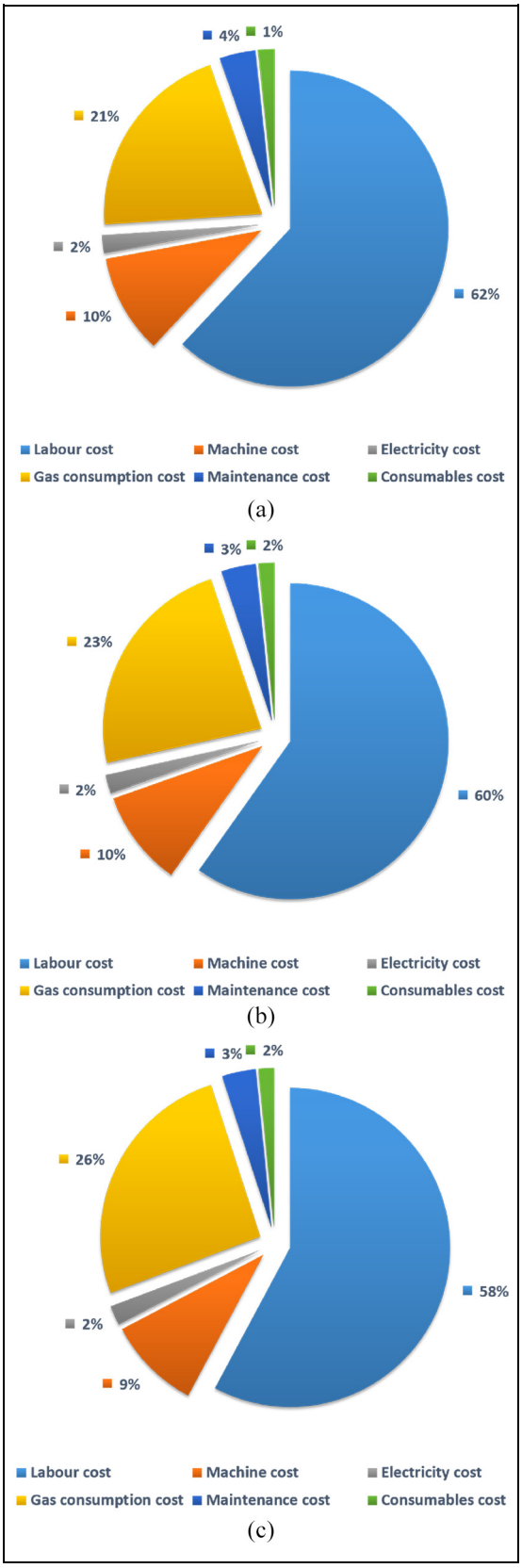

Figure 4. Percentage contribution of cost components in the total drilling cost at (a) low level: $P_e = 20$ J, $P_d = 6$ ms, $G_p = 50$ psi, $G_{fr} = 30$ mm^3/s (b) medium level: $P_e = 30$ J, $P_d = 11$ ms, $G_p = 75$ psi, $G_{fr} = 35$ mm^3/s and (c) high level: $P_e = 40$ J, $P_d = 16$ ms, $G_p = 100$ psi, $G_{fr} = 40$ mm^3/s of process parameters.

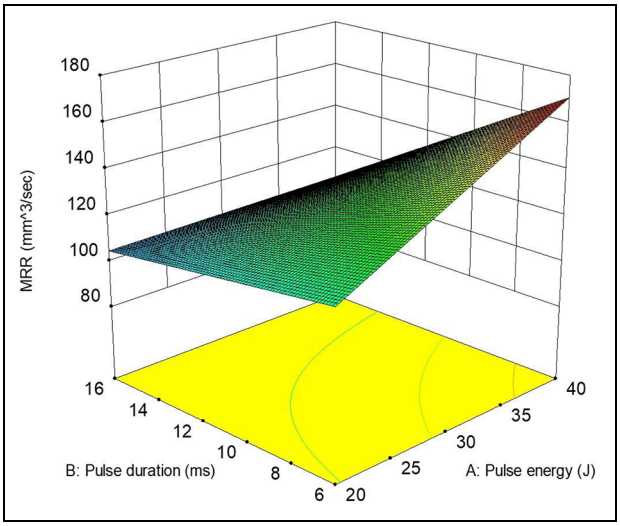

Figure 5. Surface plot for MRR: P_e versus P_d.

Investigation

To examine the individual and simultaneous influence of input process parameters, that is, pulse energy, pulse duration, gas pressure and gas flow rate on MRR, hole quality and drilling cost, 3D surface plots were drawn and are provided below.

Influence of pulse energy and pulse duration on MRR. Figure 5 illustrates the effects of pulse energy and pulse duration on MRR. It is observed that MRR is more sensitive to a change in pulse duration as compared to pulse energy. Furthermore, MRR increases with increase in pulse energy. This is due to the fact that high pulse energy increases the melt surface temperature, which in turn enhances recoil pressure. This ultimately results in high MRR. On the other hand, higher MRR is observed at low values of pulse duration because peak power of the laser beam is higher when a short pulse duration is employed, which helps in penetration during the laser drilling operation and results in an increase in the material removal rate. Similar results are noted by Yang et al.[40] and Sarfraz et al.[15]

Influence of gas pressure and gas flow rate on MRR. The surface plot of MRR (Figure 6) based on gas pressure and gas flow rate shows that MRR is maximum at high level of gas flow rate. Because higher gas flow rate provides additional thermal energy to support the heating phenomena due to the oxidising nature of compressed air. MRR is found increasing with increase in gas pressure, because higher the pressure greater the kinetic force of gas that efficiently expels the molten material outside the hole cavity. Pattanayak and Panda[41] and Panda et al.[19] reported the similar results. It is also

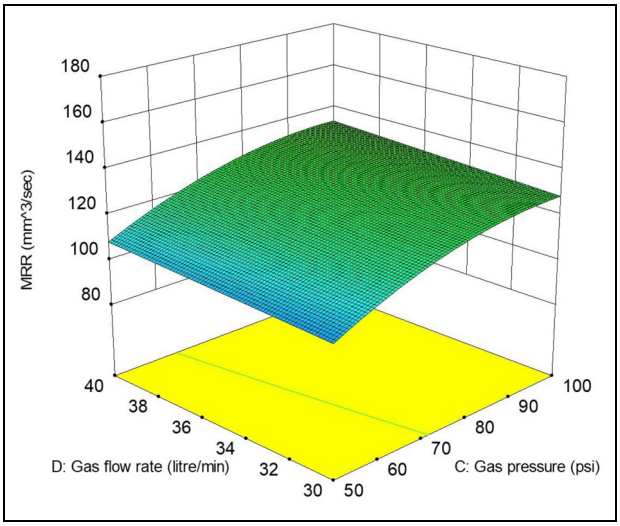

Figure 6. Surface plot for MRR: G_p versus G_{fr}.

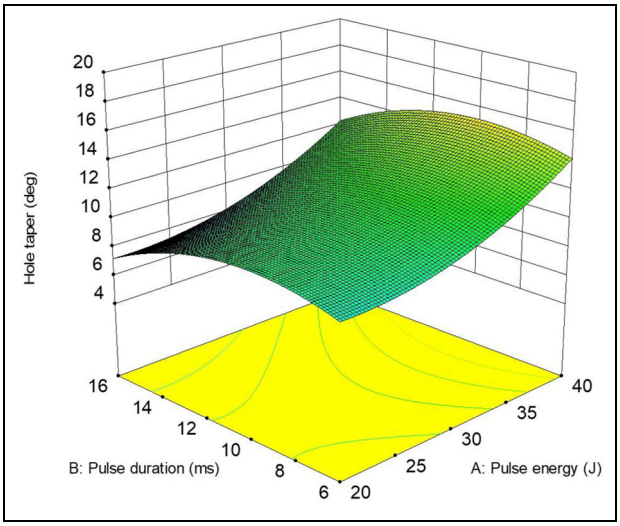

Figure 7. Surface plot for hole taper: P_e versus P_d.

evident that MRR is more influenced by gas pressure than the gas flow rate.

Influence of pulse energy and pulse duration on hole taper. The relationship between the effects of pulse energy and pulse duration on hole taper is illustrated in Figure 7. There is a noticeable increase in hole taper with an increase in pulse duration up to a specific limit. Further, hole taper starts to decrease at higher levels of pulse duration because of sufficient laser beam-work piece interaction time. On the other hand, maximum hole taper is obtained at high values of pulse energy. This is because a high pulse energy laser beam melts and vaporizes the material (top) surface instantly that creates a large (entrance) hole diameter. The intensity of the laser beam decreases due to diffraction as it penetrates, which increases the hole taper. Similar findings have been observed by Sarfraz et al.[15] and Chatterjee et al.[42]

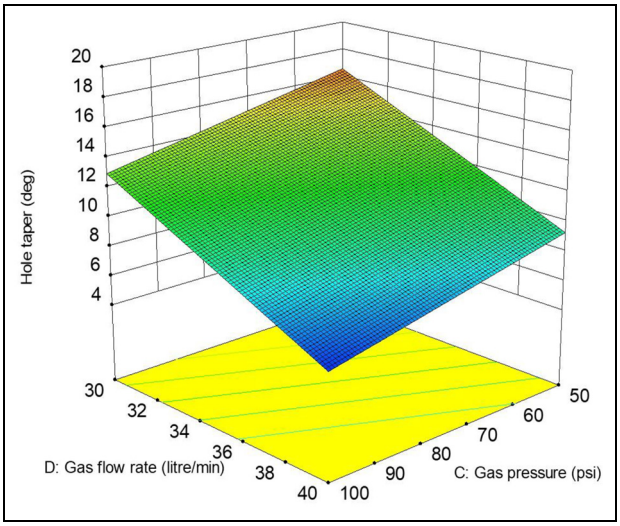

Figure 8. Surface plot for hole taper: G_p versus G_{fr}.

Influence of gas pressure and gas flow rate on hole taper. The effects of gas pressure and gas flow rate on hole taper are revealed in Figure 8. Hole taper decreases with increase in gas pressure. This is because higher gas pressure properly removes the molten metal from the material (top) surface. Moreover, an increase in pressure does not permit the molten metal to set down inside the hole cavity. Thus, hole taper reduces when higher gas pressure is used which is in accordance with the findings of Chatterjee et al.[42] A similar trend has been observed with the increase in gas flow rate because higher compressed air flow rate increases the localised temperature due to its combustible supportability and results in efficient removal of the material from the hole exits which results in lower hole taper, as stated by Nawaz et al.[20]

Influence of pulse energy and pulse duration on drilling cost. Figure 9 illustrates the response of pulse energy and pulse duration on drilling costs. The lowest value of drilling cost is observed at minimum values of pulse duration and pulse energy. This increase in drilling cost at higher pulse duration and pulse energy values results from an increase in drilling time and power consumption respectively.[33] The response graph also indicates that pulse duration has more influence than pulse energy.

Influence of gas pressure and gas flow rate on drilling cost. The effects of gas pressure and gas flow rate on drilling costs are described in Figure 10. An increase in gas flow rate shows a noticeable increase in drilling cost, whereas no prominent effect is observed from gas pressure. Higher gas flow rate results in more gas consumption, which ultimately increases drilling cost.

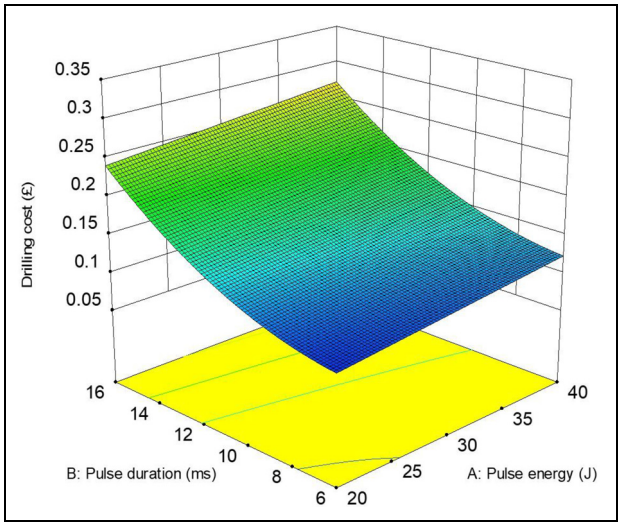

Figure 9. Surface plot for drilling cost: P_e versus P_d.

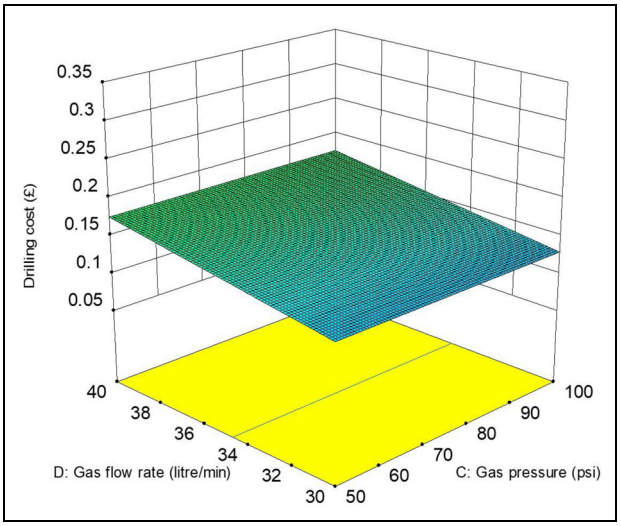

Figure 10. Surface plot for drilling cost: G_p versus G_{fr}.

Riveiro et al.[39] and Eltawahni et al.[33] noticed the same results for the CO_2 laser cutting process.

Optimisation

Different methods and techniques are available to solve single-response optimisation. However, these procedures cannot be used when multiple responses are involved and the optimal combination of process parameters is desired. Generally, in multi-responses, the response parameters are conflicting; for instance, lower hole taper is achieved with high pulse duration and high gas flow rate but increase in pulse duration and gas flow rate affect the cost. To mitigate these problems, RSM based Grey rational analysis (GRA) was used to perform multi-objective optimisation aiming to maximise the MRR while minimising hole taper and drilling cost. In GRA, the first step is "grey relational generating," where normalisation is carried-out on the collected responses to develop the range between 0 and 1. According to the desired target for the responses, such as MRR (maximisation in target), cost and hole taper (minimisation in target) relations are defined. For MRR, "larger-the-better" is the desirable target, so the following relation (equation (13)) is used:

$$x_i(y) = \frac{x_i^0(y) - min\left(x_i^0(y)\right)}{max(x_i^0(y) - min(x_i^0(y))} \tag{13}$$

Here, $x_i(y)$ is the grey relational generation value and $x_i^0(y)$ is the y th response value collected for the i th experiment, where $i = 1, 2, 3, \ldots, l$ and $y = 1, 2, \ldots, m$ with $l = 27$ and $m = 3$.

However, "smaller-the-better" is the desired target for cost and hole taper. That is why the desired target is defined in the following relation (equation (14)):

$$x_i(y) = \frac{max(x_i^0(y) - x_i^0(y)}{max(x_i^0(y) - min(x_i^0(y))} \tag{14}$$

Here, $max(x_j^0(y))$ is the maximum value and $min(x_j^0(y))$ is the minimum value of the particular response.

In the second step, grey relational coefficients (GRC) are determined to develop a relationship between real experimental normalised values and the desirable data. The grey-relational coefficient is defined by equation (15):

$$\mathrm{a}_i(y) = \frac{\Delta_{min} + \zeta\,\Delta_{max}}{\Delta_{0i}(y) + \zeta\,\Delta_{max}} \tag{15}$$

Here, $\mathrm{a}_i(y)$ is the GRC value, $\Delta_{0i}(y)$ is the normalised response value, Δ_{min} and Δ_{max} are the minimum and maximum absolute differences. Zeta (ζ) is a distinguish coefficient restricted between 0 and 1. The principal objective of applying ζ is to lower the effect of Δ_{max}. When the value of Δ_{max} is too big it significantly affects the GRC. In this study, zeta (ζ) is selected as 0.5 to fit the practical needs.[43]

The grey-relational-grade (GRG) is determined as the weighted sum of GRC. Finally, GRG is calculated using equation (16).

$$\gamma_i = \sum_{y=1}^{n} \omega_y\,\mathrm{a}_i(y) \tag{16}$$

Here γ_i is the final GRG value of each experiment, n denotes the number of responses (MRR, cost, hole taper) and ω_y is the normalised weight of response y. The highest GRG depicts the best parameter combination for the desired targets.

Based on the conflicting responses, grey relation entropy method[44] was used to assign the weights to each response to avoid human-made assumptions. In this way, a realistic weight calculation method is used systematically. This method assigns weight based on the influence of process parameters on the response, where higher weight is allocated to the response with a higher variation.

Table 4. Weight assignment using the grey relation entropy method.

Parameters	MRR				H_T				C_d			
	Level 1	Level 2	Level 3	R	Level 1	Level 2	Level 3	R	Level 1	Level 2	Level 3	R
P_e	0.394	0.477	0.584	0.189	0.641	0.618	0.428	0.213	0.695	0.621	0.578	0.118
P_d	0.639	0.461	0.381	0.258	0.566	0.547	0.680	0.132	0.824	0.632	0.420	0.404
G_P	0.390	0.505	0.518	0.128	0.511	0.566	0.687	0.176	0.660	0.629	0.595	0.065
G_{fr}	0.461	0.482	0.503	0.042	0.420	0.562	0.789	0.368	0.671	0.634	0.569	0.102
$\sum R$				0.617				0.890				0.689
Weight				0.281				0.405				0.314

Table 5. Response table for normalised, GRC and GRG values.

Exp. No.	Normalised values			GRC			GRG
	MRR	H_T	C_d	MRR	H_T	C_d	
1	0.195	0.771	0.805	0.383	0.355	0.686	0.497
2	0.251	0.723	0.749	0.4	0.75	0.643	0.609
3	0.465	1	0.535	0.483	0.493	1	0.695
4	0	0.229	1	0.333	0.667	0.393	0.462
5	0.064	0.731	0.936	0.348	0.466	0.65	0.508
6	0.228	0.645	0.772	0.393	0.336	0.585	0.453
7	0.351	0.984	0.649	0.435	0.702	0.97	0.735
8	1	0.819	0	1	0.443	0.734	0.717
9	0.141	0.314	0.859	0.368	0.669	0.422	0.484
10	0.178	0.336	0.822	0.378	0.493	0.429	0.435
11	0.408	0.683	0.592	0.458	0.523	0.612	0.541
12	0.436	0.758	0.564	0.47	0.498	0.674	0.561
13	0.47	0.707	0.53	0.485	0.493	0.631	0.547
14	0.216	0.847	0.784	0.389	0.461	0.765	0.564
15	0.535	0.692	0.465	0.518	0.333	0.619	0.501
16	0.617	0.861	0.383	0.566	0.425	0.782	0.609
17	0.263	0.574	0.737	0.404	0.471	0.54	0.480
18	0.258	0.715	0.742	0.403	0.891	0.637	0.651
19	0.632	0.506	0.368	0.576	0.541	0.503	0.535
20	0.822	0.857	0.178	0.737	0.623	0.777	0.717
21	0.212	0	0.788	0.388	0.928	0.333	0.535
22	0.515	0.715	0.485	0.507	0.477	0.637	0.550
23	0.682	0.769	0.318	0.611	0.712	0.684	0.672
24	0.288	0.259	0.712	0.412	0.851	0.403	0.546
25	0.317	0.814	0.683	0.423	0.658	0.729	0.621
26	0.715	0.661	0.285	0.637	0.425	0.596	0.554
27	0.532	0.54	0.468	0.516	1	0.521	0.670

Firstly, the mean value of GRC was calculated at each level of the process parameter associated with the individual response (Table 4). For example, at level 1 of pulse energy, the mean value of GRC for MRR was determined as 0.394. The maximum and minimum values of the mean of GRC were then used to calculate the range, as shown in equation (17).

$$R_{i,j} = max\{Q_{i,j,1}, Q_{i,j,2}, \ldots Q_{i,j,u}\} - min\{Q_{i,j,1}, Q_{i,j,2}, \ldots Q_{i,j,u}\} \quad (17)$$

where $R_{i,j}$ is the range of mean value of GRC ($Q_{i,j}$) for the response i, process parameter j with level u.

The value of weight ω for each response is calculated using equation (18).

$$\omega_i = \sum_{i=1}^{c} R_{i,j} / \sum_{i=1}^{c} \sum_{j=1}^{p} R_{i,j} \quad (18)$$

Where c is the number of responses and p is the number of process parameters.

Table 5 depicts the normalised, grey relational coefficients and grey relational grade values for the corresponding responses. It is evident that test no. 7 depicts the highest value of GRG. Therefore, the seventh experiment gives the optimum condition for higher MRR with lower hole taper and cost.

Further, the mean value of GRG was also calculated for each level of the drilling parameter and is provided in Table 6. Moreover, the total mean of GRG for all experiments is calculated as 0.572 (Table 6). Each row

Table 6. GRG response table at each level of process parameters.

Process parameters	GRG		
	Level 1	Level 2	Level 3
Pulse energy	**0.594**	0.580	0.532
Pulse duration	**0.691**	0.557	0.491
Gas pressure	0.537	0.574	**0.602**
Gas flow rate	0.534	0.569	**0.620**

Total mean value of GRG = 0.572.

Table 7. Confirmatory test results.

Conditions	Initial drilling conditions	Optimal drilling conditions
Levels	P_e1-P_d1-G_p2-$G_{fr}2$	P_e1-P_d1-G_p3-$G_{fr}3$
MRR (mm^3/s)	118.2	130.4
H_T (deg)	7.91	4.52
C_d (£)	0.00818	0.00921
GRG	0.735	0.791
Improvement in GRG value	0.056	
% improvement in GRG	7.62%	

presents the process parameter and its levels. The level of the corresponding process parameter with the highest value of GRG is presented in bold form (Table 6). For instance, 0.594 is the highest value of GRG for pulse energy. Therefore, the optimum parameter levels for higher MRR and lower hole taper and cost are P_e1-P_d1-G_p3-$G_{fr}3$.

The ANOVA was performed for GRG to evaluate the significance of each process parameter. The results are provided in Appendix 4. The percentage contribution of each process parameter in GRG was also computed. Pulse duration was found as the most significant parameter with a 60% contribution that affects the MRR, hole taper, and cost followed by gas flow rate (11%), gas pressure (6.5%) and pulse energy (5.5%).

Confirmatory test

A confirmation test has been done for verification of improvement in the responses. The levels of process parameters selected for the confirmation test are shown in Table 7. The initial drilling conditions represent test No. 7 (optimum parameters from Table 5) and the optimal drilling conditions represent the optimum parameter levels from Table 6. The estimated value of GRG for optimal drilling condition (γ_{es}) was determined using equation 19.

$$\gamma_{es} = \gamma_x + \sum_{i=1}^{q} (\gamma_o - \gamma_x) \tag{19}$$

where γ_x is the total mean value of GRG, γ_o is the mean value of GRG at optimal drilling condition and q denotes the number of process parameters. Table 7 shows a 7.6% improvement in GRG when optimal drilling conditions are considered. This table also indicates a considerable improvement in the values of MRR and hole taper at the expense of minor cost increase because of the higher levels of gas pressure and gas flow rate used. Therefore, it can be postulated that the conflicting responses in laser drilling are improved by using RSM based GRA.

Conclusions

In the present study experimental analysis of productivity, quality and process cost is highlighted for the single-pulse laser drilling of IN 718 superalloy. The impacts of pulse energy, pulse duration, gas pressure and gas flow rate have been examined on the selected responses. Multi-objective optimisation was performed using RSM based grey rational analysis (GRA) to get the optimal combination of process parameters against the optimised response values (maximum MRR with minimum hole taper and drilling cost). In addition, detailed cost analysis has been performed to explore the economic implications of the laser drilling process. Based on the experimentation results and analysis, the main observations are listed below:

- The results of ANOVA for responses revealed all the selected process parameters as significant concerning MRR and hole taper. However, for drilling cost, pulse duration was determined to be the most effective parameter followed by gas flow rate and pulse energy.
- For best results, low pulse energy should be used with short pulse duration since high pulse duration decreases the productivity and excessive pulse energy increases the hole taper. Also, both pulse energy and pulse duration affect the cost. On the other hand, higher gas pressure and gas flow rate can be employed to minimise the hole taper and increase productivity for only a small increase in cost. In this study, the most optimum drilling conditions identified were pulse energy of 20 J, pulse duration of 6 ms, the gas pressure of 100 psi and gas flow rate of 40 mm^3/s.
- The ANOVA results for GRG depict the highest percentage contribution of pulse duration (60%) among all the process parameters. This shows that pulse duration contributed significantly during single-pulse drilling operation when the simultaneous optimisation of all responses is considered.
- Analytical cost modelling provides the economic perspective for laser drilling. The detailed cost analysis revealed labour cost, gas consumption and machine costs as the major cost elements of the laser drilling process.
- The process parameters (pulse energy, pulse duration, gas pressure, and gas flow rate) were formulated with respect to the responses (MRR, hole

taper, and cost) to develop mathematical models using regression analysis. The values of adequacy measures (R^2 and adjusted R^2) depict that the developed mathematical models are adequate and can be used to predict the output responses for the proposed drilling parameters range.

One quality attribute of the laser drilling process (hole taper) has been considered in this work. The surface integrity of laser-drilled holes can be analysed along with other response variables, such as heat-affected zone, recast layer thickness, surface roughness and circularity to improve drilling performance. Other heuristics techniques, such as NSGA-II, Artificial Bee Colony and Particle Swarm Optimisation can also be used for the analysis. Moreover, other process parameters, including nozzle diameter, nozzle stand-off distance and laser beam focal position can be considered along with different materials.

Further research is in progress to explore the economic prospects of other laser drilling processes, that is, percussion and trepanning drilling.

Acknowledgements

The authors want to thank the Punjab Educational Endowment Fund (PEEF, Pakistan) and Cranfield University (United Kingdom) for financial support of this research. The authors are also thankful to Mr Masood Habib Ahmed for proofreading this manuscript.

Declaration of conflicting interests

The author(s) declared no potential conflicts of interest with respect to the research, authorship, and/or publication of this article.

Funding

The author(s) received no financial support for the research, authorship, and/or publication of this article.

ORCID iD

Shoaib Sarfraz https://orcid.org/0000-0002-1373-2054

References

1. van Dijk MHH. Drilling of aero-engine components: experiences from the shop floor. In: D. Belforte and M. Levitt (eds) *The industrial laser handbook*. New York, NY: Springer, 1992, pp.113–118.
2. McNally CA, Folkes J and Pashby IR. Laser drilling of cooling holes in aeroengines: state of the art and future challenges. *Mater Sci Technol* 2004; 20: 805–813.
3. Kuram E and Ozcelik B. Optimization of machining parameters during micro-milling of Ti6Al4V titanium alloy and Inconel 718 materials using Taguchi method. *Proc IMechE, Part B: J Engineering Manufacture* 2017; 231: 228–242.
4. Marimuthu S, Antar M and Dunleavey J. Characteristics of micro-hole formation during fibre laser drilling of aerospace superalloy. *Precis Eng* 2019; 55: 339–348.
5. Schneider M, Girardot J and Berthe L. Recoil pressure and surface temperature in laser drilling. In: *International congress on applications of lasers & electro-optics*, Orlando, FL, 23–27 October, 2011, pp.478–481. Laser Institute of America.
6. Ng GKL, Crouse PL and Li L. An analytical model for laser drilling incorporating effects of exothermic reaction, pulse width and hole geometry. *Int J Heat Mass Transf* 2006; 49: 1358–1374.
7. Schaaf P. *Laser processing of materials: fundamentals, applications and developments*. Berlin, Heidelberg: Springer-Verlag, 2010.
8. Gautam GD and Pandey AK. Pulsed Nd: YAG laser beam drilling: a review. *Opt Laser Technol* 2018; 100: 183–215.
9. Dhar S, Saini N and Purohit R. A review on laser drilling and its techniques. In: *International conference of advances in mechanical engineering (AME 2006)*, Fatehgarh Sahib, 1–3 December 2006.
10. Bandyopadhyay S, Gokhale H, Sundar JKS, et al. A statistical approach to determine process parameter impact in Nd:YAG laser drilling of IN718 and Ti-6Al-4V sheets. *Opt Lasers Eng* 2005; 43: 163–182.
11. Schaeffer R. *Fundamentals of laser micromachining*. Boca Raton, FL: CRC Press - Taylor & Francis, 2012.
12. Bahar ND, Marimuthu S and Yahya WJ. Pulsed Nd: YAG laser drilling of aerospace materials (Ti-6Al-4V). *IOP Conf Ser Mater Sci Eng* 2016; 152: 012056.
13. Tam SC, Yeo CY, Jana S, et al. Optimization of laser deep-hole drilling of Inconel 718 using the Taguchi method. *J Mater Process Technol* 1993; 37: 741–757.
14. Marimuthu S, Antar M, Dunleavey J, et al. An experimental study on quasi-CW fibre laser drilling of nickel superalloy. *Opt Laser Technol* 2017; 94: 119–127.
15. Sarfraz S, Shehab E, Salonitis K, et al. Experimental investigation of productivity, specific energy consumption, and hole quality in single-pulse, percussion, and trepanning drilling of in 718 superalloy. *Energies* 2019; 12: 4610.
16. French P, Hand D, Peters C, et al. Investigation of the Nd: YAG laser percussion drilling process using high speed filming. In: *Laser materials processing conference ICALEO 98*, Orlando, FL, 16–18 November 1998, pp.1–10. Laser Institute of America.
17. French P, Hand D, Peters C, et al. Investigation of the Nd: YAG laser percussion drilling process using factorial experimental design. In: *Laser materials processing conference ICALEO* 99, San Diego, California, 15–18 November 1999, pp.51–60. Laser Institute of America.
18. Ezhilarasan C, Velayudham A, Nagaraj M, et al. Analysis of Hole Taper, Recast Layer and Heat Affected zone in pulsed O2 and N2 laser drilling of Difficult-to-cut alloy Nimonic C-263. *IOP Conf Ser Mater Sci Eng* 2018; 390: 012036.
19. Panda S, Mishra D and Biswal BB. Determination of optimum parameters with multi-performance characteristics in laser drilling—a grey relational analysis approach. *Int J Adv Manuf Technol* 2011; 54: 957–967.

20. Nawaz S, Kashif M, Abbas N, et al. Effect of defocused plane on entrance and exit hole geometry of high grade steel 18CrNi8 during percussion drilling by Nd: YAG millisecond laser system. *Mater Res Express* 2020; 7: 016556.
21. Yilbas BS and Yilbas Z. Parameters affecting hole geometry in laser drilling of nimonecs 75. In: *Lasers in motion for industrial applications, Proceedings of the SPIE*, 1987, pp.87–91. Los Angeles, CA: SPIE.
22. Yilbas BS. Parametric study to improve laser hole drilling process. *J Mater Process Technol* 1997; 70: 264–273.
23. Rodden WS, Kudesia S, Hand D, et al. A comprehensive study of the long pulse Nd:YAG laser drilling of multilayer carbon fibre composites. *Opt Commun* 2002; 210: 319–328.
24. Yilbas BS and Aleem A. Laser hole drilling quality and efficiency assessment. *Proc IMechE, Part B: J Engineering Manufacture* 2004; 218: 225–233.
25. Kacar E, Mutlu M, Akman E, et al. Characterization of the drilling alumina ceramic using Nd: YAG pulsed laser. *J Mater Process Technol* 2009; 209: 2008–2014.
26. Xiao L, Zhao J, Yan Z, et al. Technologic investigation of laser micro-drilling on the thin ceramic plate. *Acta Opt Sin* 2014; 34: 34.
27. Zhang T, Zhang C, Li J, et al. Formation mechanism of recast layer in millisecond laser drilling of Ti6Al4V Alloys. *Acta Opt Sin* 2017; 37: 0214001.
28. Dietrich J, Brajdic M, Engbers S, et al. Enhancing the quality and productivity of laser drilling by changing process gas parameters while processing. In: *International congress on applications of lasers & electro-optics*, Orlando, FL, 2–5 November 2009, pp.729–732. Laser Institute of America.
29. Sarfraz S, Shehab E, Salonitis K, et al. Evaluation of productivity and operating cost of laser drilling process – a case study. In: *Advances in manufacturing technology XXXII: Proceedings of the 16th international conference on manufacturing research*, 2018, pp.9–14. University of Skövde, Sweden: IOS Press.
30. Priyadarshini M, Pattnaik SK, Mishra D, et al. Multi characteristics optimization of laser drilling process parameter using grey fuzzy reasoning method. *Mater Today Proc* 2015; 2: 1518–1532.
31. Priyadarshini M, Tripathy PP, Mishra D, et al. Multi characteristics optimization of laser drilling process parameter using fuzzy-TOPSIS mmethod. *Mater Today Proc* 2017; 4: 8538–8547.
32. Benyounis KY, Olabi AG and Hashmi MSJ. Multi-response optimization of CO2 laser-welding process of austenitic stainless steel. *Opt Laser Technol* 2008; 40: 76–87.
33. Eltawahni HA, Hagino M, Benyounis KY, et al. Effect of CO2 laser cutting process parameters on edge quality and operating cost of AISI316L. *Opt Laser Technol* 2012; 44: 1068–1082.
34. Sarfraz S, Shehab E, Salonitis K, et al. An experimental investigation of productivity, cost and quality for single-pulse laser drilling process. In: *17th international conference on manufacturing research, incorporating the 34th national conference on manufacturing research*, 10–12 September 2019, pp.334–339. Queen's University, Belfast: IOS Press.
35. Montgomery DC. *Design and analysis of experiments*. 9th ed. New York: John Wiley & Sons, 2017.
36. NASA. NASA cost estimating handbook (CEH). Version 4.0, *National Aeronautics and Space Administration*, https://www.nasa.gov/offices/ocfo/nasa-cost-estimating-handbook-ceh (2015, accessed 8 January 2020).
37. D'Urso G, Quarto M and Ravasio C. A model to predict manufacturing cost for micro-EDM drilling. *Int J Adv Manuf Technol* 2017; 91: 2843–2853.
38. Shehab E and Abdalla HS. An intelligent knowledge-based system for product cost modelling. *Int J Adv Manuf Technol* 2002; 19: 49–65.
39. Riveiro A, Mejías A, Soto R, et al. CO2 laser cutting of natural granite. *Opt Laser Technol* 2016; 76: 19–28.
40. Yang Y, Chen Z and Zhang Y. Melt flow and heat transfer in laser drilling. *Int J Therm Sci* 2016; 107: 141–152.
41. Pattanayak S and Panda S. Laser beam micro drilling – a review. *Lasers Manuf Mater Process* 2018; 5: 366–394.
42. Chatterjee S, Mahapatra SS, Bharadwaj V, et al. Drilling of micro-holes on titanium alloy using pulsed Nd:YAG laser: parametric appraisal and prediction of performance characteristics. *Proc IMechE, Part B: J Engineering Manufacture* 2018; 095440541880560.
43. Sarıkaya M and Güllü A. Multi-response optimization of minimum quantity lubrication parameters using Taguchi-based grey relational analysis in turning of difficult-to-cut alloy Haynes 25. *J Clean Prod* 2015; 91: 347–357.
44. Khan A, Jamil M, Salonitis K, et al. Multi-objective optimization of energy consumption and surface quality in nanofluid SQCL assisted face milling. *Energies* 2019; 12: 710.
45. Ion J. *Laser processing of engineering materials: principles, procedure and industrial application*. Oxford: Butterworth-Heinemann, 2005.
46. Williams S. Drilling. In: Webb CE and Jones JDC (eds) *Handbook of laser technology and applications*. Bristol: Institute of Physics Publishing, 2004, pp.1633–1653.
47. Dahotre NB and Harimkar S. *Laser fabrication and machining of materials*. Boston, MA: Springer Science & Business Media, 2008.
48. Yeo CY, Tam SC, Jana S, et al. A technical review of the laser drilling of aerospace materials. *J Mater Process Tech* 1994; 42: 15–49.
49. Sarfraz S, Shehab E, Salonitis K, et al. Towards cost modelling for laser drilling process. In: *Proceedings of the 25th ISPE Inc. International conference on transdisciplinary engineering*, University of Modena and Reggio Emilia, Modena, Italy, 3–6 July 2018, pp.611–618. Amsterdam, Netherlands: IOS Press.

Appendix 1. Laser system specification.

Specifications	Values
Wavelength	1064 nm
Peak power*	9 kW
Pulse duration	0.2–20 ms
Average power*	300 W
Pulse energy*	56 J
Pulse frequency*	1000 Hz

*Maximum values.

Appendix 2. Cost drivers of the laser drilling process.

Cost Drivers	Ion[45]	William[46]	Dahotre and Harimkar[47]	Yeo et al.[48]	Sarfraz et al.[49]
Equipment running cost	Equipment depreciation Electrical consumption Replaceable components (lenses, flash lamps) Gas consumption	Equipment depreciation Electricity and water usage cost Replaceable components (lenses, laser pumps) Component handling	Equipment depreciation Component handling	Equipment depreciation Electrical consumption Replaceable components (lenses, flash lamp, filters) Gas consumption	Equipment depreciation Electrical consumption Replaceable components (lenses, flash lamp, filters, nozzle) Gas consumption Component handling
	Overhead	Overhead	Overhead		Overhead
Maintenance	Equipment maintenance	Equipment maintenance			Equipment maintenance
Material			Material cost		Material cost
Labour	Labour (laser operators and engineers) cost	Labour (operator) cost	Labour cost		Labour cost

Appendix 3. ANOVA for MRR, HT and Cd.

Source MRR	df	Sum of squares	Mean square	F value	*p* value
Model	8	9879.41	1234.93	97.65	< 0.0001
A-Pulse energy	1	2133.33	2133.33	168.69	< 0.0001
B-Pulse duration	1	4606.00	4606.00	364.22	< 0.0001
C-Gas pressure	1	1922.80	1922.80	152.05	< 0.0001
D-Gas flow rate	1	76.00	76.00	6.01	0.0247
AB	1	635.04	635.04	50.22	< 0.0001
AC	1	93.12	93.12	7.36	0.0142
BD	1	111.30	111.30	8.80	0.0083
C^2	1	301.80	301.80	23.87	0.0001
Residual	18	227.63	12.65		
Lack of Fit	16	214.58	13.41	2.06	0.3764
Pure Error	2	13.05	6.52		
Cor Total	26	10107.04			
R^2		0.9775	Adj R^2		0.9675
H_T					
Model	6	330.35	55.06	42.97	< 0.0001
A-Pulse energy	1	78.29	78.29	61.09	< 0.0001
B-Pulse duration	1	10.42	10.42	8.13	0.0099
C-Gas pressure	1	39.28	39.28	30.65	< 0.0001
D-Gas flow rate	1	160.27	160.27	125.07	< 0.0001
A^2	1	12.48	12.48	9.74	0.0054
B^2	1	21.40	21.40	16.70	0.0006
Residual	20	25.63	1.28		
Lack of Fit	18	25.28	1.40	8.08	0.1156
Pure Error	2	0.35	0.17		
Cor Total	26	355.97			
R^2		0.9280	Adj R^2		0.9064
C_d					
Model	5	0.087	0.017	61.23	< 0.0001
A-Pulse energy	1	0.00291	0.00291	10.23	0.0043
B-Pulse duration	1	0.067	0.067	234.94	< 0.0001
D-Gas flow rate	1	0.006533	0.006533	22.97	< 0.0001
BD	1	0.005099	0.005099	17.93	0.0004

(continued)

Appendix 3. Continued

Source MRR	df	Sum of squares	Mean square	F value	*p* value
B^2	1	0.005716	0.005716	20.10	0.0002
Residual	21	0.005972	0.0002844		
Lack of Fit	19	0.005784	0.0003044	3.25	0.2616
Pure Error	2	0.0001876	0.00009379		
Cor Total	26	0.093			
R^2		0.9358	Adj R^2		0.9205

Appendix 4. ANOVA for GRG.

Source	df	Sum of squares	Mean square	F value	*p*-value	% Contribution
Model	4	0.17	0.042	30.52	< 0.0001	
Pulse energy	1	0.011	0.011	8.26	0.0088	5.5
Pulse duration	1	0.12	0.12	88.32	< 0.0001	60
Gas pressure	1	0.013	0.013	9.24	0.0060	6.5
Gas flow rate	1	0.022	0.022	16.25	0.0006	11
Residual	22	0.030	0.001365			
Lack of fit	20	0.030	0.001491	14.16	0.0680	
Pure error	2	0.0002107	0.0001053			
Cor total	26	0.20				

2020-11-03

An integrated analysis of productivity, hole quality and cost estimation of single-pulse laser drilling process

Sarfraz, Shoaib

Sage

Sarfraz S, Shehab E, Salonitis K, et al., (2020) An integrated analysis of productivity, hole quality and cost estimation of single-pulse laser drilling process. Proceedings of the Institution of Mechanical Engineers, Part B: Journal of Engineering Manufacture, Volume 235, Issue 14, þÿ D e c e m b e r 2 0 2 1 , p p . 2 2 7 3 2 2 8 7

https://doi.org/10.1177/0954405420968161